Journal of Environmental Management 393 (2025) 127197

Contents lists available at ScienceDirect

Journal of Environmental Management

journal homepage: www.elsevier.com/locate/jenvman

Research article

GEDI and Sentinel data integration for quantifying agroforestry tree height and stocks

Giovanni D'Amico [a], Elia Vangi [a,b,*], Martin Schwartz [c], Francesca Giannetti [a], Saverio Francini [d], Piermaria Corona [e], Walter Mattioli [e], Gherardo Chirici [a,f]

[a] geoLAB - Laboratoy of Forest Geomatics, Department of Agricultural, Food, Environmental and Forestry Sciences and Technologies, University of Florence, via San Bonaventura 13, I-50144, Florence, Italy
[b] Forest Modelling Laboratory, Institute for Agriculture and Forestry Systems in Mediterranean, National Research Council of Italy (CNR-ISAFOM), Perugia, Italy
[c] Laboratoire des Sciences du Climat et de l'Environnement, LSCE/IPSL, CEA-CNRS-UVSQ, Université Paris Saclay, 91191, Gif-sur-Yvette, France
[d] Department of Science and Technology of Agriculture and Environment (DISTAL), University of Bologna, 40126, Bologna, Italy
[e] CREA - Research Centre for Forestry and Wood, via Valle della Quistione 27, I-00166, Rome, Italy
[f] Fondazione per il Futuro delle Città, Firenze, Italy

ARTICLE INFO

Handling Editor: Dr. Lixiao Zhang

Keywords:
Agroforestry
Carbon stock
GEDI
Poplar plantation
Sentinel
Remote sensing

ABSTRACT

Agroforestry is a strategic asset for combating climate change and mitigating the environmental impacts of agricultural intensification, offering a nature-based solution for enhancing landscape resilience. In particular, poplar plantations contribute to the development of ecological networks within homogeneous agricultural landscapes, while also producing high-demand plywood and sequestering CO_2 in durable manufactured goods. Monitoring short-rotation poplar plantations requires frequent updates, which are infeasible with conventional National Forest Inventories (NFIs). Remote sensing (RS) has emerged as a highly effective tool for monitoring the structural variables of poplar plantations. This study aims to estimate the carbon stocks of poplar plantations in the Padan Plain, which spans approximately 46,000 km^2 in northern Italy. To achieve this, we developed a 10m high-resolution canopy height model (CHM) using a deep learning U-Net approach, with Sentinel-1 and Sentinel-2 multi-band imagery as predictors for GEDI waveforms derived tree height. The U-Net CHM for 2021 was evaluated with external validation data from NFI plots, achieving a mean absolute error of 2.6 m. Using annual poplar plantations data in the survey area, along with a poplar-specific yield table derived from terrestrial laser scanning, we applied the U-Net CHM to predict key forestry variables, including diameter at breast height (DBH), growing stock volume (GSV), aboveground biomass (AGB), and carbon stock (CS) in all stands. Results were compared with external validation data from NFI, yielding RMSE values of 30.7 %, 46.2 %, and 63.2 % for DBH, GSV, and AGB, respectively. Meanwhile, independent field surveys produced RMSE values of 19 % and 37.7 % for DBH and GSV, respectively. The average GSV estimated was 70 m^3 ha^{-1}, while total CS were 12 MgC ha^{-1}. Based on poplar plantation maps for 2021 and 2022, we estimated the total harvested GSV of poplar trees to be 370,000 m^3, equal to 66,000 MgC. The corresponding average harvested area was 1.5 ha, with an average yield of 130 m^3 per hectare. The integration of multiple RS datasets with advanced machine learning techniques facilitates the effective monitoring of dynamic poplar plantations, for both mapping purposes and quantifying key forest variables relevant to climate change mitigation, such as carbon stocks.

1. Introduction

Agroforestry refers to land-use systems in which trees are grown in combination with agriculture on the same land (European Commission, 2014). These systems have gained renewed attention in Europe as a strategic asset for addressing climate change and mitigating the environmental impacts of agricultural intensification while also providing a nature-based solution for enhancing landscape resilience (Golicz et al., 2022; FOREST EUROPE, 2018). However, not all EU countries adopt the same definition of agroforestry (Golicz et al., 2022). As a result,

* Corresponding author. GeoLAB - Laboratoy of Forest Geomatics, Department of Agricultural, Food, Environmental and Forestry Sciences and Technologies, University of Florence, via San Bonaventura 13, I-50144, Florence, Italy.
E-mail address: elia.vangi@unifi.it (E. Vangi).

https://doi.org/10.1016/j.jenvman.2025.127197
Received 4 April 2025; Received in revised form 20 August 2025; Accepted 3 September 2025
Available online 10 September 2025

practices considered agroforestry in one country or region may be classified as either forestry or agricultural activities in other EU countries and regions (Burgess and Rosati, 2018). Notably, the role of agroforestry in carbon sequestration remains understudied (Corona et al., 2023; C-FARMs, 2023).

The Padan Plain in northern Italy is one of Europe's most intensively cultivated agricultural regions (D'Amico et al., 2021; Romano et al., 2024). Trees play a crucial role in mitigating pollutants and improving environmental quality in these agricultural landscapes. This mitigation function is partly fulfilled through agroforestry activities, particularly those focused on fruit and timber production. Poplar (*Populus* spp.) is critical in this region. As a fast-growing species, it is widely cultivated in specialized plantations for timber production, with rotations of 10–12 years for plywood production (Corona et al., 2024; Nervo et al., 2024). Poplar plywood is in high demand across various industries, making poplar plantations strategically important as a nature-based solution at the EU level (Freer-Smith et al., 2019). The rapid growth of poplar enables the storage of significant amounts of CO_2 over a short period, enhancing soil sequestration (Antoniella et al., 2024; Feng et al., 2020), creating ecological networks, and mitigating climate change by locking carbon in durable products. Additionally, poplar plantations help reduce the pressure on natural forests by meeting the global demand for forest products (Feng et al., 2020; Freer-Smith et al., 2019; Łukaszkiewicz et al., 2024).

However, these plantations are highly dynamic, and accurate, reliable, and timely monitoring updates are crucial for managing them effectively (Bergante, 2022; D'Amico et al., 2021). In particular, canopy characteristics such as height are considered crucial (Romano et al., 2024), as they enable a range of assessments related to ecosystem services (Abelleira et al., 2016), carbon stock quantification (Karna et al., 2015), wildlife management (Hyde et al., 2006), and sustainable forest management (Wulder et al., 2008). Canopy height is directly correlated with both ecological and site-specific indicators (e.g., site quality, climate conditions), as well as stand variables such as stand age, primary productivity, above ground biomass, Leaf Area Index (LAI), and canopy cover (Torres de Almeida et al., 2022).

Modern land monitoring systems are based on proximal and remote sensing technologies, enabling the investigation of tree canopy characteristics in a robust and replicable manner, which significantly improves monitoring compared to traditional fieldwork (Romano et al., 2024). Different technologies are suitable such as terrestrial cameras (Romano et al., 2024; Chianucci et al., 2020), UAV photogrammetric data (Romano et al., 2024; Chianucci et al., 2020), terrestrial laser scanning (Puletti et al., 2021), airborne laser scanning (Tompalski et al., 2019), and satellite stereo mapping (Liu et al., 2019). However, the limited range of technologies, such as UAVs, terrestrial LiDAR (Light Detection and Ranging), and cameras, restricts their effectiveness in farm-level investigations. For large-scale assessments, these tools are often inadequate. At the same time, options like LiDAR from Airborne Laser Scanning (although capable of covering vast areas) are typically cost-prohibitive for regular monitoring, even on an annual basis, to track plantation dynamics. A recent study by Liu et al. (2019) addressed this limitation, creating a canopy height map in flat areas using stereo and multispectral data from the Chinese satellite ZY3-02. However, these sensors are mainly only locally available nowadays, severely limiting their application. Understanding canopy height variation is essential for polar plantation management, especially in the Po Valley, where the increased frequency and severity of drought events related to climate change potentially compromises the canopy structure and growth rate of poplar plantations (Romano et al., 2022; Baronetti et al., 2022).

Emerging opportunities arise using satellite data. Among these, Sentinel-1 (S1) radar data, Sentinel-2 (S2) multispectral optical data, and spaceborne LiDAR data from the Global Ecosystem Dynamics Investigation (GEDI) mission are particularly promising, as they were developed specifically for land and environmental monitoring and are freely available. The two S1 polar-orbiting satellites provide global coverage of Synthetic Aperture Radar (SAR) operating in the C-band. This wavelength proves useful due to its greater dynamic range of backscattering (Dalponte et al., 2023). Whilst, the S2 mission provides high spatial resolution optical data, featuring bands with a resolution of up to 10 m and a dense time series, offering high spectral resolution with ten bands useful for vegetation investigation. The revisit time varies from two to five days, depending on the latitude. Notably, GEDI was the first LiDAR satellite mission, specifically designed to recover vertical vegetation structures and collect innovative data on vegetation since April 2019 aboard the International Space Station (ISS). Providing 25-m resolution forest height measurements in tropical and temperate forests (51.6° N to 51.6° S latitude). GEDI is equipped with a waveform LiDAR that consists of three lasers, generating eight transects (beams) of forest structural information.

Although all sensor data have been used to create various forest-related products, integrating multiple sensor data appears to be the most effective approach. Accordingly, GEDI forest height measurements have been combined with Landsat data to produce a global forest canopy height model (CHM) map with a 30-m spatial resolution for 2019 (Potapov et al., 2021). Lang et al. (2023) generated a global canopy height map with a 10-m resolution predicting the GEDI RH98 (relative height, i.e., the height below which 98 % of the returned pulse energy is received) footprint based on S2 imagery. Pauls et al. (2024) used S1 and S2 cloud-free data, along with GEDI RH100, in a fully convolutional neural network to generate high-resolution (10 m) global-scale CHM. Other studies have developed regional 10-m canopy height models (CHMs) using S2 and aerial LiDAR data (Astola et al., 2021; Fayad et al., 2024). Recently, GEDI data were combined with LiDAR data to train self-supervised learning and vision transformer models based on Maxar optical imagery, producing high-resolution (1 m) CHM (Tolan et al., 2024).

To monitor the changes in poplar plantations — not only for creating plantation maps but also for quantifying key variables essential for assessing the impact of climate change mitigation, such as carbon stock — the integration of multiple remote sensing datasets which providing timely, comprehensive and frequently updated data together with advanced machine learning approaches are crucial. Deep learning (DL) techniques have proven particularly promising in this context. Among these, Convolutional Neural Networks (CNNs) offer powerful tools that enable remote sensing research to handle large volumes of training data, resulting in more accurate outcomes, particularly for image interpretation tasks. CNNs can learn multi-scale image features, such as texture, which can be used for making predictions (Dalagnol et al., 2022; Illarionova et al., 2022).

Several datasets were available in our extensive survey area. First, annual poplar plantation maps were developed through semi-automatic classification of remote sensing (RS) images, which were then refined through photointerpretation of high-resolution orthophotos (D'Amico et al., 2021). Second, an allometric equation for poplar tree volume was developed using terrestrial LiDAR data (Chianucci et al., 2020). However, combining these datasets with sophisticated new methods has yet to be fully explored.

In this study, a DL model that leverages GEDI's height data as a reference to estimate poplar plantation carbon stocks was implemented.

This represents the first application of a U-Net architecture to map poplar plantations, in which GEDI height data were integrated with S1 and S2 images to create a 10-m resolution, wall-to-wall CHM (Schwartz et al., 2023, 2024). Using these poplar plantation maps and a poplar-specific yield table, growing stock volume (GSV), aboveground biomass (AGB), and carbon stock (CS) were estimated across all plantations.

2. Materials

2.1. Survey area

The survey area is the Northern Italy Padan Plain (45° N; 10° E), where most Italian agroforestry plantations are located (Corona et al., 2020; D'Amico et al., 2021). The Po Valley is the largest river basin in Italy. It is highly populated and represents the most important economic area of Italy. The study was conducted in 330,000 ha of agricultural areas in five administrative Regions, distinguished by various crops, horticultural practices, and forest tree crops (Fig. 1). Specifically, plantations of specialized poplar, other broadleaf trees, polycyclic and sporadic broadleaf trees coppice, and a few coniferous stands are present.

2.2. Remote sensing data

2.2.1. Sentinel-1

S1 is a SAR mission operating in the C-band, consisting of two Sentinel satellites (S1A and S1B), launched by the European Space Agency (ESA) in 2014 and 2016, respectively, with a 12-day repeat cycle in a sun-synchronous orbit.

We utilized Ground Range Detected (GRD) scenes with dual-band cross-polarization (Vertical-Vertical and Vertical-Horizontal bands at 10-m resolution). The S1 toolbox, which includes radiometric calibration, terrain orthorectification, and thermal noise removal, was used to preprocess these scenes in the Google Earth Engine (GEE) cloud computing platform (Gorelick et al., 2017). The S1 dataset provides backscattering coefficients (dB), which quantify the microwave radiation reflected back towards the radar system after being emitted.

On the GEE platform, we selected all images from the survey area over a five-month period in 2021 (from May 1, 2021, to October 1, 2021). Images from the ascending and descending orbits were divided by computing the median of the pixels in the image time series. The median is minimally sensitive to extreme values, reducing the impact of moisture effects in soil and vegetation that might be present in raw S1 data. Four 10 m resolution composites were created, two in VV and VH, ascending and descending, respectively, and scaled to a range of 0–1 to match the S2 input data's range of values (Schwartz et al., 2024).

2.2.2. Sentinel-2

S1 and S2's mission is included in the ESA Copernicus Earth Observation programme. The two S2 satellites (nowadays the mission includes the third operational Sentinel-2C satellite not used here) feature a wide-swath width of 290 km, with 13 high spectral resolution bands Multi-Spectral Imaging (MSI) sensor, and a varying spatial resolution of 10 m, 20 m, and 60 m (Drusch et al., 2012). All images with a processing level of L2A (i.e., atmospherically corrected surface reflectance images) from the exact timing as the S1 images (2021-05-01 to 2021-10-01) with cloud cover of less than 50 % were selected using the cloud mask to create a per-pixel median composite image in GEE. Spectral bands with 20 m resolution were resampled to 10 m. Finally, to improve the training of an artificial neural network, the input S2 data were linearly scaled to a range of values from 0 to 1, similar to S1.

2.2.3. GEDI

The GEDI sensor is mounted on the ISS. It provides 25-m resolution forest height measurements in tropical and temperate forests (between latitudes 51.6° N and S), generating eight transects of structural data (Dubayah et al., 2021; Francini et al., 2022; Vangi et al., 2023a). GEDI data was available in various products based on preprocessing levels, where the L1B product corresponded to the energy return waveforms. Here, as a reference variable to generate a continuous 10-m resolution height map, the L2A products were used, which provided metrics such as canopy relative height (RH). Specifically, we used the RH95, which demonstrated a better correlation with other height sources than RH_{100} (Potapov et al., 2021).

In total, to cover the entire survey area in 2021, 1,371,490 pulses were downloaded from NASA's EarthDataSearch site from the GEDIv002 L2A product (Dubayah et al., 2021). Some of these were excluded due to atmospheric reasons, filtering out appropriate flags such as quality_flag set to zero. (2) toploc, botloc, or num_detectedmodes, RH_{100} provided metrics had a null value (Fig. 1).

The Train, Validation, and Test datasets were subsequently created by spatially separating these GEDI pulse traces. Specifically, the 653,100 km^2 tiles that covered the survey area were randomly split into 453 Train tiles, 114 Validation tiles, and 86 Test tiles, representing 70 %, 17 %, and 13 % of the GEDI footprints, respectively. We used the train tiles to train the model (See Section 3.1), the validation tiles to monitor

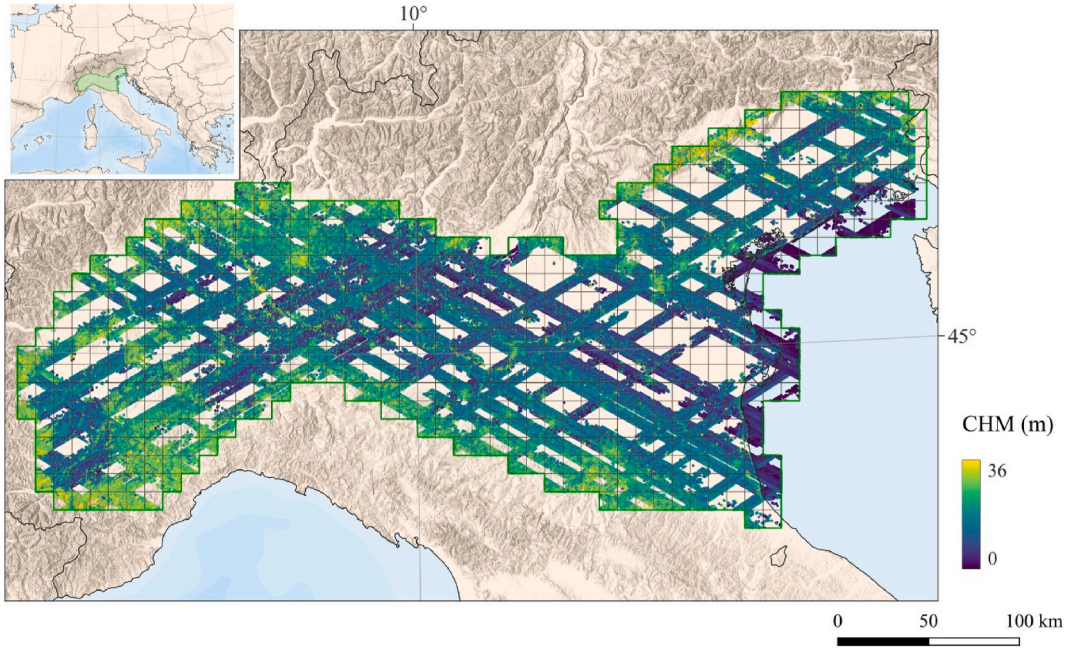

Fig. 1. GEDI RH95 pulses overview and survey area tiles.

the model performances during the training phase, and the test tiles to carry out a final assessment of the model performance. As ground-truth reference data were available for this study area (Section 2.4), we did not use these test tiles in the results part of this study.

2.3. Global canopy height model maps

To evaluate the quality of our U-Net CHM model, we compared tree heights with those from three global height maps developed in independent studies (Lang et al., 2023; Potapov et al., 2021; Tolan et al., 2024). Maps from Potapov et al. (2021), Lang et al. (2023), and Tolan et al. (2024) are based on optical data and GEDI pulse. Using Landsat-8 data to infer tree height from GEDI pulses via a bagged regression trees ensemble approach, Potapov et al. (2021) provided a global CHM for 2019 at a 30-m resolution (https://glad.umd.edu/dataset/gedi/). Lang et al. (2023) created a 2020 global wall-to-wall canopy height map at a scale of 10-m by using S2 data to calculate canopy height from GEDI footprints using a deep fully convolutional network (https://langnico.github.io/globalcanopyheight/). Meanwhile, Tolan et al. (2024) employed self-supervised learning and vision transformer approaches, utilizing Maxar high-resolution optical imagery calibrated with GEDI data and airborne LiDAR to produce a 1-m high-resolution CHM map (https://gee-community-catalog.org/projects/meta_trees/).

2.4. Reference data

2.4.1. Field truth dataset

The field reference data for the survey area was derived from the third Italian National Forest Inventory (Gasparini et al., 2022) fieldwork. For each plot, field-measured data for individual trees are freely accessible online (https://www.inventarioforestale.org/). Data for 35 circular 530-m^2 NFI field plots were measured in the survey area of the poplar plantations. The sample number is due to the random selection of NFI plots and the small spatial extent of plantations, which comprise about 1 % of the total Italian forest area (Gasparini et al., 2022). However, the plot distribution throughout the study area and the diversity in measured data ensure the proper representation of plantations.

Based on single-tree data measured in the field, the plot average height was calculated as the average height of the trees with the average basal area. Aggregate GSV and AGB data were also used to assess the accuracy of the poplar stock. Despite the NFI reference year 2015, ground data were acquired between April 2018 and April 2019. The temporal difference between ground data and predicted map appears to be sufficiently small. However, due to the high dynamism of poplar plantations, one plot was excluded from the analysis as it had been harvested.

In addition, 60 square plots of 50 × 50 m (equivalent to 2500 m^2), with traditional forestry field surveys (such as DBH, tree height, and associated GSV per individual tree), were conducted between 2020 and 2021 (Chianucci et al., 2021).

2.4.2. Poplar plantation mapping

Poplar plantation polygon reference datasets (reference years 2021 and 2022) were obtained by updating the poplar map of northern Italy, which was derived from a semi-automatic classification approach using a fully connected neural network and S2 images (D'Amico et al., 2021). These datasets were refined through photointerpretation using high-resolution orthophotos. Precisely, the poplar polygons mapped for 2021 encompassed more than 13,000 plantations, totaling approximately 30,000 ha. By updating the map to 2022, cut poplar plantations were also identified, totaling approximately 4000 ha.

3. Methods

3.1. U-net model

The U-Net model, initially designed for biomedical image segmentation (Ronneberger et al., 2015), is a DL model that belongs to the CNN category. It comprises a series of convolution operations to extract relevant features from an image. Its "U" shape is due to an ascending and descending path that gives the model a multi-scale overview of an image. Thus, the model can capture both fine-scale features and the broader general context that contribute to the final prediction. Here, we adapted the PyTorch version of the U-Net proposed by Milesi (https://github.com/milesial/PyTorch-UNet) for a regression task involving S1 and S2 images as predictors and GEDI's RH95 heights as labels, following previous studies (Schwartz et al., 2023). The model's encoder–decoder structure with skip connections facilitates the extraction of multi-scale features. This multi-scale capability is crucial in capturing fine-scale canopy details and broader contextual information, thereby enhancing tree height estimation accuracy compared to traditional deep learning methods. The model parameters from Schwartz et al. (2023) served as a starting point, and they were then refined through training on the Train tiles of our survey area, as described in Section 2.2.3. This training was performed on the train tiles (See Section 2.2.3) using a learning rate of 0.001 with the Adam optimizer (Kingma and Ba, 2014), implemented in PyTorch. The GEDI footprints located in the validation tiles were used to follow the model performances outside of its training area and evaluate the convergence of the training. The test GEDI footprints were then used to obtain a final evaluation of the model's performances.

3.2. Tree height map validation and comparison

To validate the canopy height map, we compared the mean value of our 10-m pixels that overlap the NFI's circular plots with a radius of 13 m, which is equivalent to the mean of about 5 pixels. The map accuracy was compared in terms of MAE and RMSE%, which were calculated as the percentage of RMSE against the mean official values.

$$MAE = \frac{1}{n}\sum_{i=1}^{n}|y_i - \hat{y}_i|, \quad (1)$$

$$RMSE = \sqrt{\frac{\sum_{i=1}^{n}(y_i - \hat{y}_i)^2}{n}}, \quad (2)$$

where n is the number of field measured NFI plots, y_i is the i-th mean height associated with the plots and $\hat{y}_i$ is the i-th height predicted by the tree height map. Our height prediction was also compared with three different canopy height maps: Potapov et al. (2021), Lang et al. (2023), and Tolan et al. (2024). For each CHM dataset, the values corresponding to the spatial extent of the NFI plots were extracted and used for comparison, ensuring consistency across datasets and enabling a direct evaluation against field-based reference measurements.

3.3. Poplar stock estimation and accuracy assessment

The height prediction model provided data for the entire survey area, including every poplar polygon mapped within it. Accordingly, using the poplar-specific yield table, the growing stock volume (GSV) for each plantation stand was estimated. In particular, the equations from Chianucci et al. (2020), which were carried out using terrestrial laser scanner data from plantations included in our survey area, were used. We tested all available equations for GSV estimation, finding the best results with preliminary diameter estimation and then applying the two-entry power model.

$$DBH = \log\left(\frac{\frac{(27.61-h)+1.3}{h\times 5.97} - 1.3 \times 5.97}{-0.095}\right), \quad 3$$

$$GSV = exp(-7.74) DBH^{2.11} \times h^{0.09}, \quad 4$$

Although these equations were initially developed for single-tree measurements, given the homogeneity of poplar plantations and the standard tree spacing of 36 m^2 (6 × 6 m) (Corona et al., 2018), we can quantify DBH and GSV corresponding to 10 m of the final pixel. Next, GSV estimation was used to estimate AGB (Mg d.m. (dry matter) ha^{-1}) based on poplar wood basal density as follows:

$$AGB = GSV \times BEF \times WBD \quad 5$$

where GSV is the calculated growing stock volume, BEF (biomass expansion factor) is the category-specific biomass expansion factor (dimensionless), and WBD (wood basal density) is the wood basal density (Mg d.m. m^{-3}). In particular, BEF and WBD are those already applied by Vangi et al., 2023b, which for poplar plantation stands are equal to 1.2 and 0.29, respectively. Finally, the 2021 poplar plantation carbon stocks (CS) (MgC ha^{-1}) were obtained using the default carbon fraction factor of 0.47 from AGB (IPCC, 2006).

To assess the accuracy of GSV, AGB, and CS poplar plantation estimations, we calculated the RMSE by comparing them with the NFI and square plot field truth datasets. Since we had the poplar plantation mappings for the years 2021 and 2022, we were able to identify cut poplar plantations and thus available wood for industrial activities. For these plantations, we estimated the central stock values based on GSV, AGB, and CS maps.

4. Results

4.1. Canopy height model

The predicted U-Net CHM, trained using S1 and S2 predictors and sparse GEDI reference data, was produced for the whole study area. Due to the variability of agroforestry's spatial and temporal distribution in agronomic environments, an accurate forest mask is lacking and, therefore, has not been applied. However, the U-Net CHM visual inspection enables the differentiation of agroforestry plantation cover from other land uses (Fig. 2).

4.1.1. Evaluation with independent datasets

For the 35 NFI plots, the height predictions at the pixel level ranged between 4.6 and 24 m, with a standard deviation of 5.1 m, while the original NFI values varied from 4.1 to 27.2 m, with a standard deviation of 6 m. The comparison between the predicted height and the NFI field truth dataset yields an R^2 coefficient of 0.63 (MAE = 2.7 m, RMSE = 22.6 %).

The comparison with the NFI dataset is reported in Fig. 4, where a strong correlation with our canopy height is evident. Moreover, the most discordant data are for the oldest INFC plots, acquired in 2018. Thus, as the estimates refer to 2021, these differences are explained mainly by the rapid growth of poplars.

4.1.2. Comparison with other canopy height maps

For the U-Net CHM evaluation, we compared the height predictions with the already available height models of Potapov et al. (2021), Lang et al. (2023), and Tolan et al. (2024). Typically, forest plantations are surrounded by non-forested land use, mainly crops. From a visual comparison, the forest stands of U-Net CHM had higher homogeneity. Slightly noisier appears to be the product in Lang et al. (2023), presumably due to a filter applied to the CHM, while in Potapov's product,

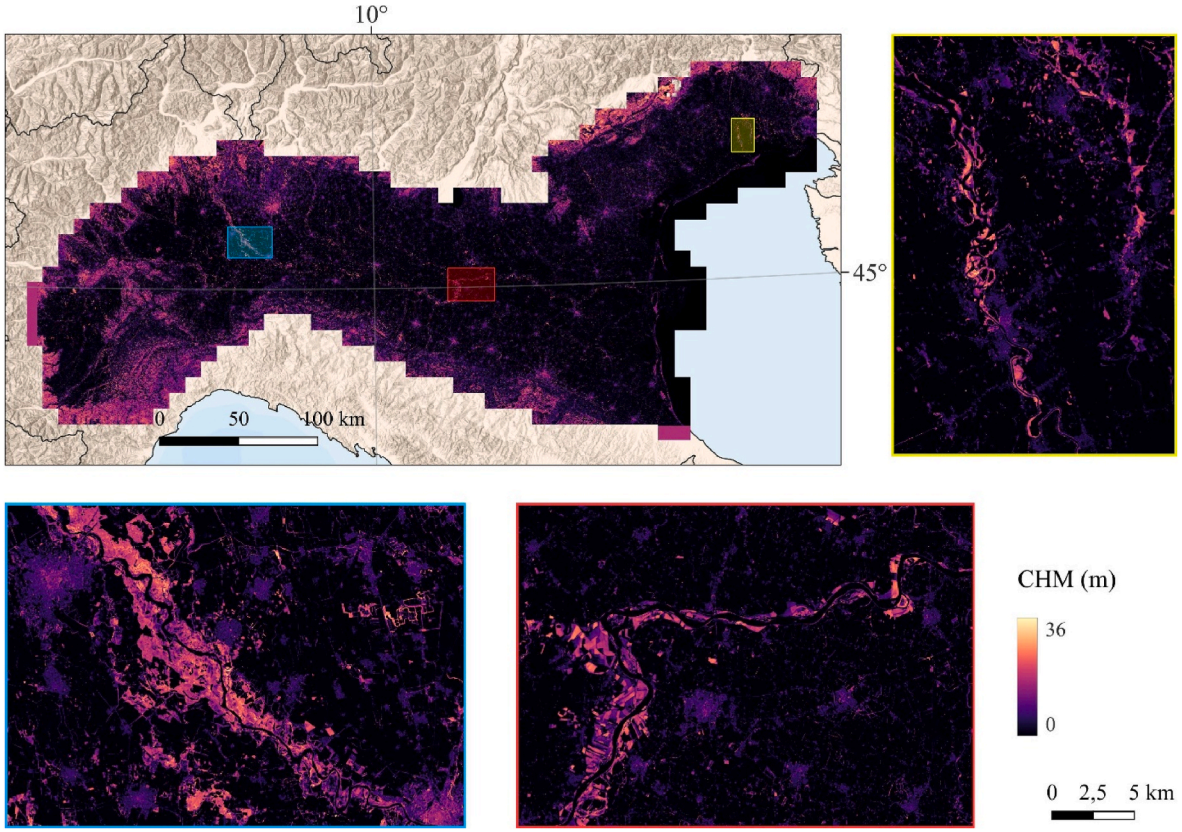

Fig. 2. Wall-to-wall forest canopy height (U-Net CHM) map of Padan Plain for 2021. In the boxes, there are three areas with extensive poplar plantations.

the borders of the various land uses appear poorly defined, partly because of the lower spatial resolution. In Tolan et al. (2024), where the pattern is always recognizable, greater diversity, even within plantations, was evident (Fig. 3).

Additionally, a comparison between the NFI data and the four CHMs analyzed is presented in Fig. 4. The U-Net CHM exhibits the strongest relationship, with the highest R^2 of 0.63, followed by Tolan et al. (2024) with an R^2 of 0.49, which reveals an overestimation of values. In contrast, the CHM of Lang et al. (2023) yields an R^2 of 0.16, whereas Potapov et al. (2021) achieve an R^2 of 0.07. In terms of RMSE, the U-Net CHM reached 3.7 m, corresponding to 22.6 % of the mean observed height, while Tolan et al. (2024), Lang et al. (2023), and Potapov et al. (2021) reached 9.9, 5.9, and 12.8m, respectively (corresponding to 60.2, 35.9, and 78.2 % of the measured height, respectively).

4.2. Poplar stocks

Considering the U-Net CHM accuracy, we used it to estimate the

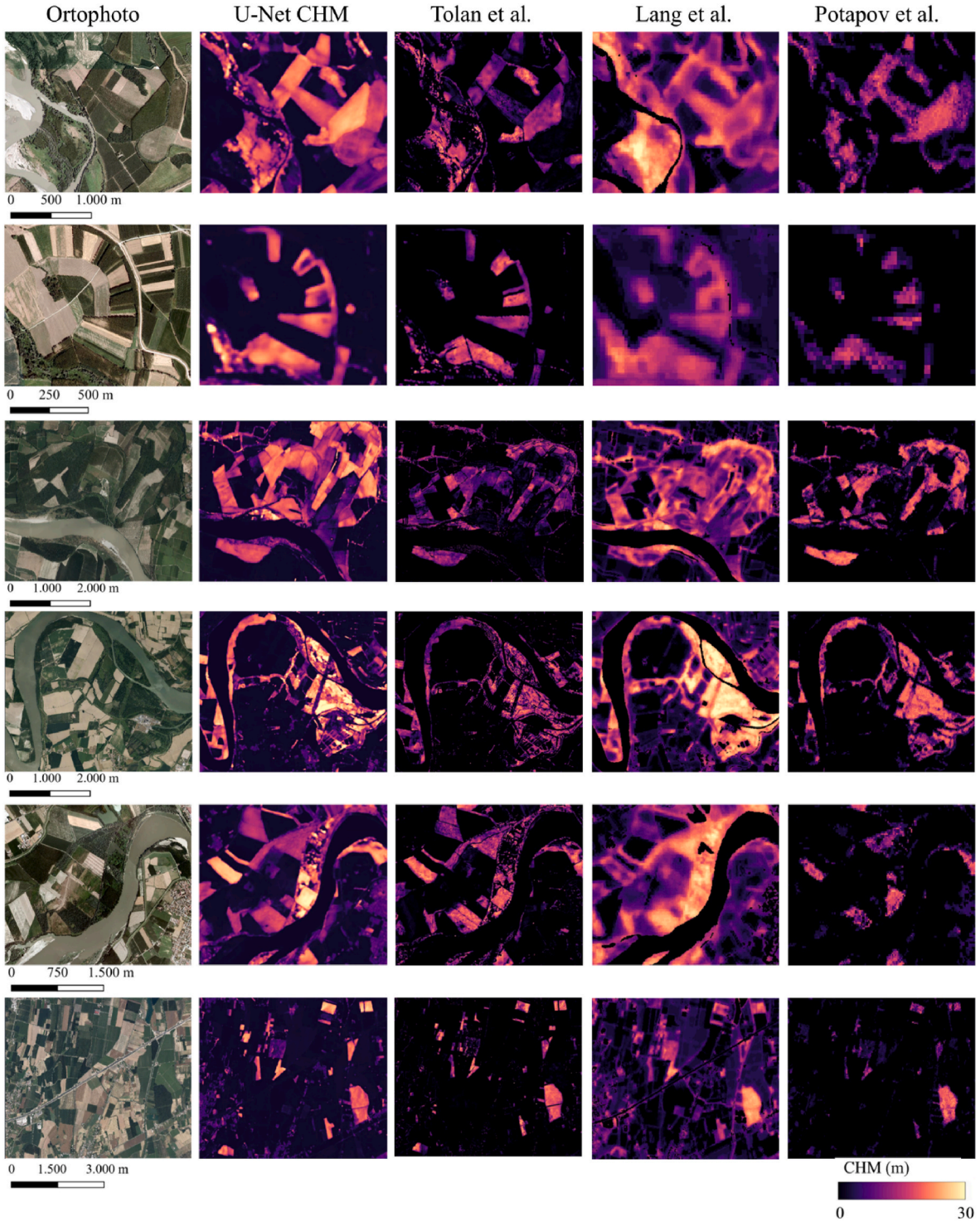

Fig. 3. Visual comparison at different scale of U-Net CHM data (10 m resolution) and three other products Tolan et al. (2024) (2024 - 1 m resolution), Lang et al. (2023) (2021 - 10 m resolution), and Potapov et al. (2021) (2019 - 30 m resolution).

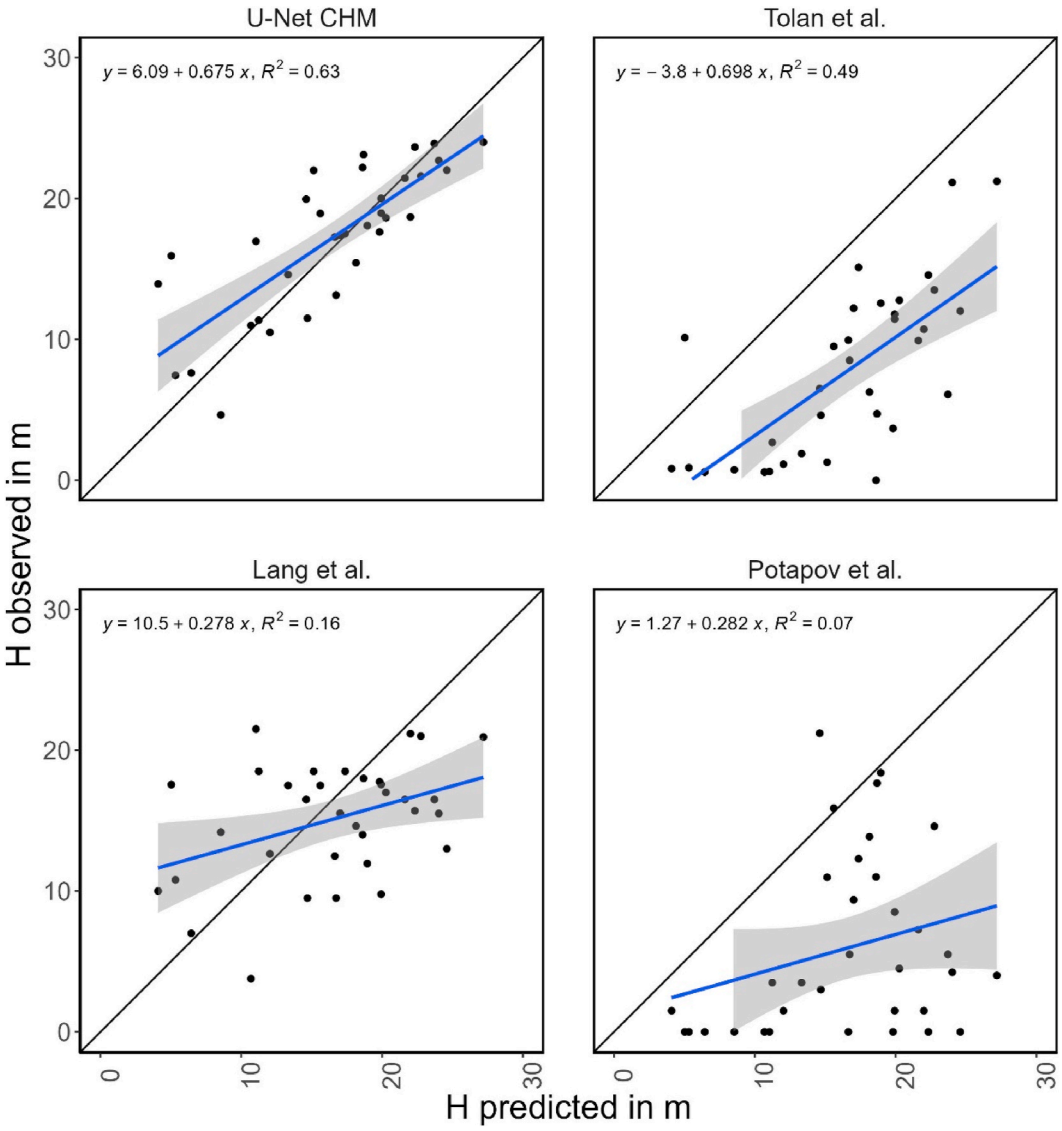

Fig. 4. Quantitative comparison of U-Net CHM data and three other products Tolan et al. (2024), Lang et al. (2023), and Potapov et al. (2021) with the NFI data in poplar plantations. The black line represents the 1:1 line.

poplar plantation stocks. Estimates of GSV and AGB were compared with ground truth data measured in the NFI and square areas (Figs. 5 and 6). The CS was excluded from the comparison since it is derived directly from the AGB values. Similarly, we focused on GSV for comparison with square plots, as AGB was derived from GSV values by applying Equation (5). A comparison with DBH data, derived from U-Net CHM using Equation (3), was also included.

Comparison with NFI data for DBH, GSV, and AGB yields RMSE values of 30.7 %, 46.2 %, and 63.2 %, respectively (Fig. 5). The comparison reveals a relatively strong relationship for GSV, while AGB appears to be slightly underestimated.

Comparison with independent field truth data in the 50 × 50 cells shows consistent values for DBH and GSV, with RMSE values of 19 % and 37.7 %, respectively (Fig. 6).

From the extraction of the stocks on the poplar stands mapped in the year 2021 (Fig. 7), the total GSV, AGB and C stock were 1,956,588.1 m^3, 703,589.1 Mg and 351,794.5 MgC, respectively, while the average GSV, AGB and C stock were 66.28 m^3 ha^{-1}, 23.83 Mg ha^{-1} and 11.92 MgC ha^{-1}, respectively.

We also extracted the three stocks within the harvested poplar stands between 2021 and 2022 to calculate the average and total harvested stock for that year. For a total harvested area of 4372 ha, we obtain a total harvested GSV of 36,9012.5 m^3, corresponding to 132,697 Mg of AGB and 66,348.52 MgC of C stock. The average GSV removed within the stands was 68.24 m^3 ha^{-1}, corresponding to 24.53 Mg ha^{-1} and 12.26 MgC ha^{-1} of AGB and C stock, respectively.

5. Discussion

This study deepens our understanding of the poplar plantations, the leading supplier of Italian wood products for industrial use. For estimating poplar stocks, we used mapping data for poplar plantations in northern Italy for 2021 and 2022. Although this data was supported by semi-automatic mapping approaches (D'Amico et al., 2021), it still required a time-consuming process of photointerpretation. The U-Net CHM we developed in this study was applied for the first time to monitor poplar plantations by integrating Sentinel and GEDI data, demonstrating its usefulness for advancing knowledge in agroforestry systems, which, with further research, could also lead to more detailed mapping.

Poplar plantations are dynamic systems, showing both spatial and growth variations from year to year. Comparisons with NFI data confirm the high dynamism of these plantations. The most significant biases,

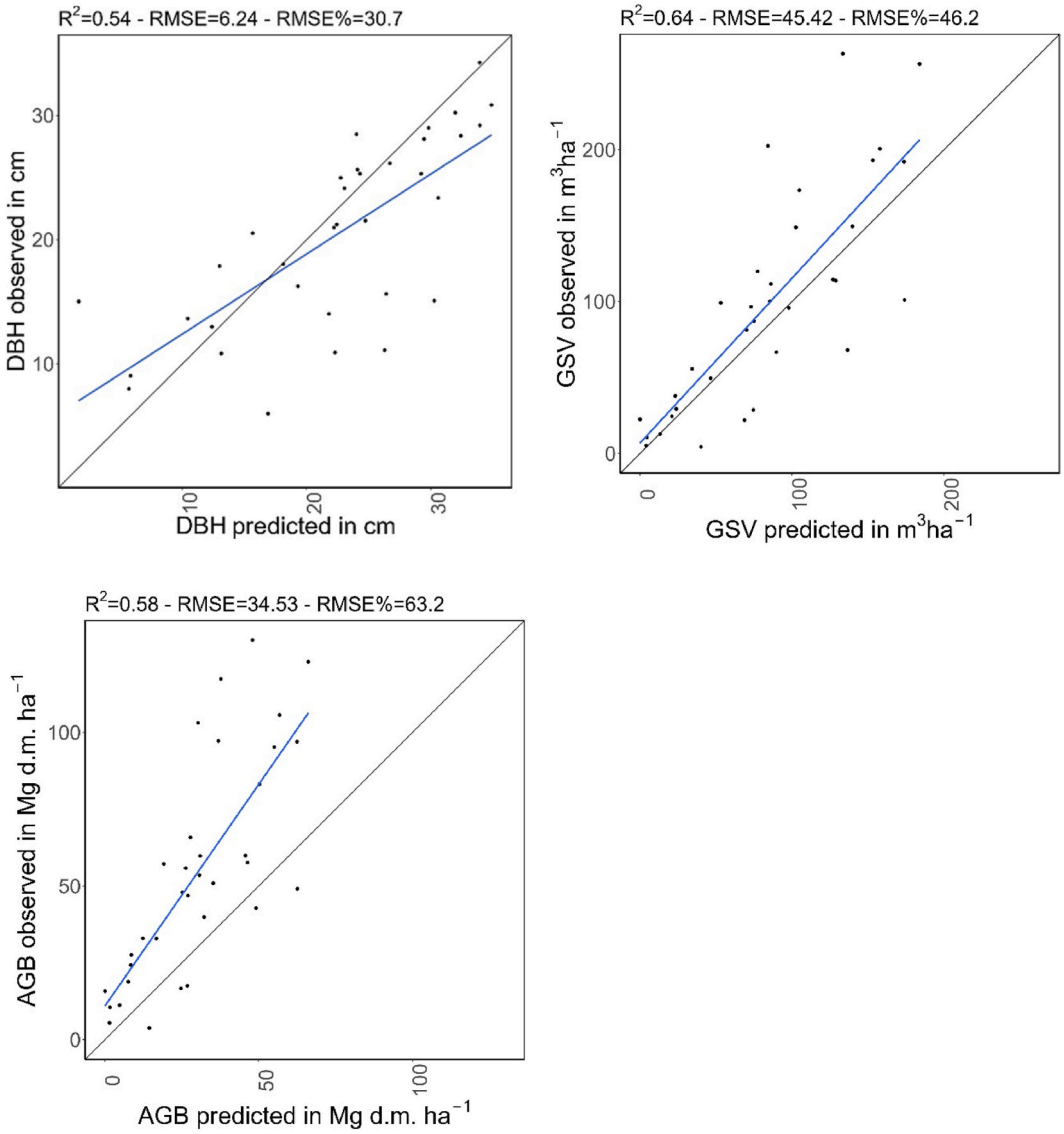

Fig. 5. Comparison of DBH, GSV, and AGB against the Italian NFI data field truth dataset in poplar plantations.

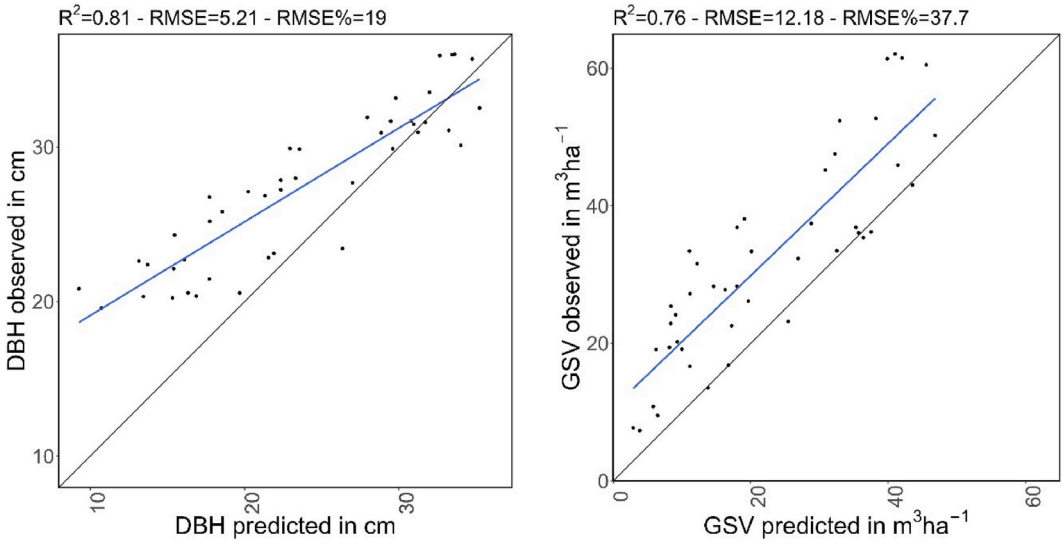

Fig. 6. Comparison of GSV against the square plot field truth dataset in poplar plantations.

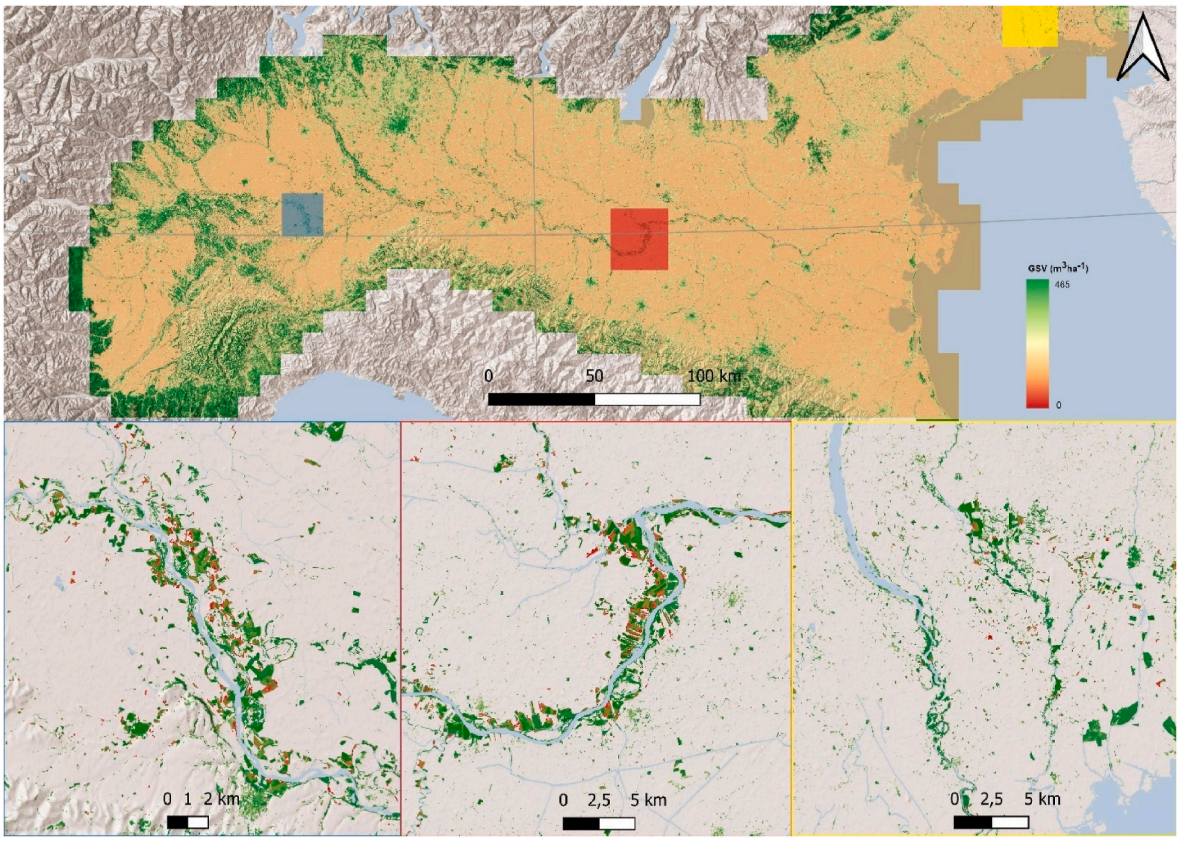

Fig. 7. Poplar plantation GSV map of Padan Plain at 10 m resolution for 2021. In the boxes, there are three areas with extensive poplar plantations.

typically overestimations, were observed in plots measured in 2018. These discrepancies may be partially attributed to natural growth between the NFI survey and the development of the U-Net CHM for the nominal year of 2021. Notably, the growth rates of poplar plantations in the Po Valley, expressed as mean annual increments, are among the highest in temperate zones, potentially exceeding 25 m^3 ha^{-1} yr^{-1} (Spinelli et al., 2011; Pra et al., 2019). The new Italian NFI is expected to provide annual estimates, enhancing the temporal resolution of forest data in Italy. However, the sparse and systematic distribution of NFI field plots remains poorly suited for monitoring intensively managed and spatially clustered systems such as poplar plantations, highlighting the need for complementary remote sensing approaches (D'Amico et al., 2025, in press).

According to our maps, an estimated 380,000 m^3 of timber were harvested and made available to the market in 2021. While this amount is significant, it is noticeably lower than the figures reported in other studies. Considering the growth of the Italian poplar cultivation sector in recent years, our data align with Zanuttini et al. (2021), who reported Italian poplar plywood production for 2017 at approximately 270,000 m^3.

Accurate spatial data on growing stock, biomass and carbon are essential for guiding forest management practices, including harvest scheduling, yield forecasting, and resource allocation (Herold et al., 2019). Moreover, reliable estimates of plantation stocks are critical for shaping evidence-based policies at national and regional levels, particularly in the context of land-use planning, timber supply chain optimization, and the sustainable development of the forest-based bioeconomy (Corona et al., 2018).

LiDAR data are recognized as essential for quantifying forest stocks (Nilsson et al., 2017; Chirici et al., 2020; D'Amico et al., 2022). However, frequent airborne LiDAR surveys remain expensive. For example, wall-to-wall airborne laser scanning data in Italy is still unavailable. This lack of data and the derived forest variables map have created limitations for validating the estimated CHM and poplar stocks. Liu et al. (2019) mapped the canopy height of poplar plantations, achieving an RMSE of 1.58 m, despite the field validation samples having a maximum height of only approximately 10 m. This study utilized the ZY3-02 satellite, which was specifically developed for China's civil space infrastructure (Xu et al., 2017). However, Chinese Earth observation satellites remain underutilized globally, with vegetation-related applications primarily driven by sensors on American or European satellites (Zhang et al., 2023). To address these limitations, integrating Sentinel data with satellite LiDAR data can provide more detailed and accurate information. Our results confirm the significant potential of integrating multiple data sources for enhanced mapping.

Since this study focused on estimating poplar plantation stocks, we selected three international CHMs for comparison with the U-Net CHM we produced. Among the many available CHMs (such as Pauls et al., 2024; Astola et al., 2021; Fayad et al., 2024), we used the datasets from Potapov et al. (2021), Lang et al. (2023), and the recent dataset from Tolan et al. (2024), which, with a 1 m resolution, represents a new generation of global height models.

A comparative analysis of the U-Net CHM and the three additional canopy height maps available across the survey area highlighted the potential of our product. Visual inspection in six representative contexts (Fig. 3) demonstrated that the U-Net CHM effectively delineated the boundaries of poplar plantations, with greater consistency and spatial clarity. The CHM by Lang et al. (2023), while comparable in resolution (10 m), exhibited more noise outside plantation areas but provided a relatively accurate representation of low-stature vegetation, tending to overestimate shorter canopies and underestimate taller ones. In contrast, the coarser-resolution CHM by Potapov et al. (2021) (30 m) lacked spatial detail and was less effective in capturing fine-scale height variation. The high-resolution product by Tolan et al. (2024) (1 m) showed clear separation between poplar plantation and adjacent areas but revealed internal variability within plantations that was not always

consistent with their structural homogeneity. These visual patterns generally align with those reported by Moudrý et al. (2024).

However, our quantitative analysis produced contrasting results: both Potapov et al. (2021) and Tolan et al. (2024) showed a systematic overestimation of canopy height in our study area, while Lang et al. (2023) yielded comparatively lower errors. These discrepancies likely stem from differences in forest type and context. Moudrý et al. (2024) evaluated CHMs across diverse natural and semi-natural forests around the globe, whereas our study focused on intensively managed poplar plantations in the Po Valley, characterized by short rotation cycles, rapid growth, and structural homogeneity. Such conditions make this forest system particularly sensitive to spatial resolution and temporal alignment between remote sensing data and reference observations, underscoring the importance of context-specific CHM validation approaches.

Given the high dynamism of poplar plantation management, the reference year of the different datasets must be considered. Referring to the NFI data, mainly surveyed in 2018, the dataset of Potapov et al. (2021), with a reference year of 2019, is the most consistent. However, it shows an evident overestimation, with the worst RMSE value of 78.2 %. The CHM from Tolan et al. (2024), derived from Maxar satellite images covering the period from 2018 to 2020, shows a clear overestimation of height, with an RMSE of 60.2 %. The CHM from Lang et al. (2023), with a reference year of 2020, yielded RMSE values of 35.9 %, whereas the U-Net CHM, with a reference year of 2021, achieved the lowest RMSE of 22.6 %. Although we were aware of the survey dates for the NFI plots and the reference years for the CHMs, we avoided adding uncertainty factors by harmonizing the analyses to a common year using the poplar increment (Schelhaas et al., 2018).

At the national level, biomass datasets are also available. Giannetti et al. (2022) developed AGB maps at a 23 m resolution based on the second Italian NFI with a reference year of 2005. At the global scale, several maps have been developed, such as the biomass map at a 300 m resolution for 2010 by Spawn et al. (2020) or the product by Santoro et al. (2021) for 2010 at a 1 ha resolution. The GEDI L4B product, based on data acquired between 2019 and 2021, provides a global AGB map at a 1 km resolution (Duncanson et al., 2022). Biomass maps have also been produced at the European scale, based on various input data and modeling approaches. Avitabile et al. (2024) recently released maps of forest area, biomass stocks, and their availability for wood supply in 2020, including statistics on gross and net volume increments from 2010 to 2020. However, several studies have highlighted differences in estimates (Araza et al., 2023) and systematic deviations from ground reference data, mainly due to their limited global coverage (Duncanson et al., 2019). Therefore, locally developed maps, such as our U-Net CHM, validated with independent datasets, remain the most reliable for local studies (Giannetti et al., 2023).

Satellite LiDAR data, particularly from the GEDI and ICESat-2 missions, are now fundamental sources of information (Guerra-Hernández et al., 2024; Varvia et al., 2024). The upcoming EDGE mission holds promise for advancing our understanding of complex forest systems, such as poplar plantations and agroforestry. While these data are beneficial and promising, they do have limitations. Products developed by integrating GEDI data with other remote sensing data can be affected by the GEDI measurement uncertainty of approximately 10-m in determining the ground location (Dubayah et al., 2020). Specifically, GEDI footprints near forest boundaries may capture bare ground outside the forest and vice versa (Schwartz et al., 2024). Moreover, the survey area has a relatively flat environment; however, in more morphologically complex regions, such as Italian forests, developing similarly accurate CHMs will require additional efforts.

6. Conclusion

The renewed prominence of agroforestry in the context of climate change mitigation and Green Deal policies is well-documented in a growing body of recent scholarly literature. In Italy, research efforts have primarily focused on the inventory of poplar plantations (Marcelli et al., 2020) and the development of mapping methodologies (D'Amico et al., 2021a). Additional studies have addressed the estimation of tree structural attributes (Chianucci et al., 2020; Puletti et al., 2021; Romano et al., 2024) and the assessment of tree stress conditions (Tauro et al., 2022).

The primary objective of this study was to estimate the spatial distribution of poplar plantation stocks in the Padan Plain, northern Italy. We generated maps of growing stock volume, aboveground biomass, and carbon stocks using a canopy height model developed through a deep learning U-Net framework. This model utilized multi-band imagery from S1 and S2 as inputs to predict tree height derived from GEDI pulse waveforms. The U-Net model, previously successfully applied in France (Schwartz et al., 2023, 2024), demonstrated high efficiency, outperforming other height estimation models. Specifically, the U-Net--derived canopy height model yielded an RMSE% of 22.6 % compared with NFI plot data.

Our estimates underscore the importance of poplar wood for industrial needs. Specifically, for 2021, we estimated approximately 1,956,600 m^3 of timber, corresponding to 352,000 Mg of carbon stored. Harvest estimates for 2022 indicate that poplar production in northern Italy totaled approximately 370,000 m^3, equivalent to over 130,000 Mg of AGB and 66,000 Mg of C stock.

Given the continuous availability of S1 and S2 data, the generated canopy height map can be updated on an annual basis to track changes in tree height. Consequently, the integration of Earth observation data into national forest monitoring systems enables the effective yearly monitoring of poplar plantation stocks.

CRediT authorship contribution statement

Giovanni D'Amico: Writing – review & editing, Writing – original draft, Software, Methodology, Formal analysis, Data curation, Conceptualization. **Elia Vangi:** Writing – original draft, Software, Methodology, Formal analysis, Data curation, Conceptualization. **Martin Schwartz:** Writing – review & editing, Methodology, Formal analysis, Data curation. **Francesca Giannetti:** Writing – review & editing, Validation, Data curation. **Saverio Francini:** Writing – review & editing, Data curation. **Piermaria Corona:** Writing – review & editing, Supervision, Conceptualization. **Walter Mattioli:** Writing – review & editing. **Gherardo Chirici:** Writing – review & editing, Supervision, Resources, Project administration, Funding acquisition, Conceptualization.

Declaration of competing interest

The authors declare that they have no known competing financial interests or personal relationships that could have appeared to influence the work reported in this paper.

Acknowledgement

This study was partially supported via the following projects: 1. MULTIFOR "Multi-scale observations to predict Forest response to pollution and climate change" PRIN 2020 Research Project of National Relevance funded by the Italian Ministry of University and Research (prot. 2020E52THS). 2. SUPERB "Systemic solutions for upscaling of urgent ecosystem restoration for forest related biodiversity and ecosystem services" H2020 project funded by the European Commission, number 101036849 call LC-GD-7-1-2020. 3. EFINET "European Forest Information Network" funded by the European Forest Institute Network Fund G-01-2021. 4. FORWARDS "The ForestWard Observatory to Secure Resilience of European Forests", HORIZON project funded by the European Commission, number 101084481 call HORIZON-CL6-2022-CLIMATE-01. 5. MONIFUN. H2020 project funded by the European Commission, number 101134991 call HORIZON-CL6-2023-CircBio-01-14. 6. NextGenCarbon. H2020 project funded by the European

Commission, number 101184989 call HORIZON-CL5-2024-D1-01-07. 7. NBFC "National Biodiversity Future Center" project funded under the National Recovery and Resilience Plan (NRRP), NextGenerationEU; Project code CN_00000033, adopted by the Italian Ministry of University and Research, CUP B83C22002930006. 8. Space It Up. Project funded by the Italian Space Agency and the Ministry of University and Research - Contract No. 2024-5-E.0 - CUP No. I53D24000060005.

Data availability

Data will be made available on request.

References

Abelleira Martínez, O.J., Fremier, A.K., Günter, S., Ramos Bendaña, Z., Vierling, L., Galbraith, S.M., Bosque-Pérez, N.A., Ordoñez, J.C., 2016. Scaling up functional traits for ecosystem services with remote sensing: concepts and methods. Ecology & Evoution 6, 4359–4371. https://doi.org/10.1002/ece3.2201.

Antoniella, G., Kumar, A., Chiarabaglio, PM., Scarascia Mugnozza, G., Chiti, T., 2024. Do poplar plantations enhance organic carbon stocks in arable soils? A comprehensive study from Northern Italy. J. Environ. Manag. 370 (2024), 122882. https://doi.org/10.1016/j.jenvman.2024.122882.

Araza, A., Herold, M., De Bruin, S., Ciais, P., Gibbs, D.A., Harris, N., et al., 2023. Past decade above-ground biomass change comparisons from four multi-temporal global maps. Int. J. Appl. Earth Obs. Geoinf. 118, 103274. https://doi.org/10.1016/j.jag.2023.103274.

Astola, H., Seitsonen, L., Halme, E., Molinier, M., Lönnqvist, A., 2021. Deep neural networks with transfer learning for forest variable estimation using sentinel-2 imagery in boreal forest. Remote Sens. 13 (12), 2392. https://doi.org/10.3390/rs13122392.

Avitabile, V., Pilli, R., Migliavacca, M., Duveiller, G., Camia, A., Blujdea, V., et al., 2024. Harmonised statistics and maps of forest biomass and increment in Europe. Sci. Data 11 (1), 274. https://doi.org/10.1038/s41597-023-02868-8.

Baronetti, A., Dubreuil, V., Provenzale, A., Fratianni, S., 2022. Future droughts in northern Italy: high-resolution projections using EURO-CORDEX and MED-CORDEX ensembles. Clim. Change 172, 1–22. https://doi.org/10.1007/s10584-022-03370-7.

Bergante, S., 2022. Poplar tree for innovative plantation models. Annals of Silvicultural Research 47 (1), 48–53. https://doi.org/10.12899/asr-2344.

Burgess, P.J., Rosati, A., 2018. Advances in European agroforestry: results from the AGFORWARD project. Agrofor. Syst. 92, 801–810. https://doi.org/10.1007/s10457-018-0261-3.

Chianucci, F., Puletti, N., Grotti, M., Ferrara, C., Giorcelli, A., Coaloa, D., Tattoni, C., 2020. Nondestructive tree stem and crown volume allometry in hybrid poplar plantations derived from terrestrial laser scanning. For. Sci. 66 (6), 737–746. https://doi.org/10.1093/forsci/fxaa021.

Chianucci, F., Marchino, L., Bidini, C., Giorcelli, A., Coaloa, D., Chiarabaglio, P., Giannetti, F., Chirici, G., Tattoni, C., 2021. Dataset of tree inventory and canopy structure in poplar plantations in northern Italy. Annals of Silvicultural Research 46, 93–96. https://doi.org/10.12899/asr-2177.

Chirici, G., Giannetti, F., McRoberts, R.E., Travaglini, D., Pecchi, M., Maselli, F., et al., 2020. Wall-to-wall spatial prediction of growing stock volume based on Italian national forest Inventory plots and remotely sensed data. Int. J. Appl. Earth Obs. Geoinf. 84, 101959. https://doi.org/10.1016/j.jag.2019.101959.

Corona, P., Bergante, S., Castro, G., Chiarabaglio, P.M., Coaloa, D., Facciotto, G., et al., 2018. Linee di indirizzo per una pioppicoltura sostenibile. Rete Rurale Nazionale, Consiglio per la ricerca in agricoltura e l'analisi dell'economia agraria, Roma, 978-88-99595-96-8.

Corona, P., Chianucci, F., Marcelli, A., Gianelle, D., Fattorini, L., Grotti, M., Puletti, N., Mattioli, W., 2020. Probabilistic sampling and estimation for large-scale assessment of poplar plantations in northern Italy. Eur. J. For. Res. 139 (6), 981–988. https://doi.org/10.1007/s10342-020-01300-9.

Corona, P., Di Stefano, V., Mariano, A., 2023. Knowledge gaps and research opportunities in the light of the european union regulation on deforestation-free products. Annals of Silvicultural Research 48, 87–89. https://doi.org/10.12899/asr-2445.

Corona, P., Bergante, S., Marchi, M., Barbetti, R., 2024. Quantifying the potential of hybrid poplar plantation expansion: an application of land suitability using an expert-based fuzzy logic approach. N. For. 55, 1231–1246. https://doi.org/10.1007/s11056-023-10026.

D'Amico, G., Vangi, E., Francini, S., Giannetti, F., Nicolaci, A., Travaglini, D., et al., 2021. Are we ready for a national Forest Information system? State of the art of forest maps and airborne laser scanning data availability in Italy. iFor. Biogeosci. For. 14, 144–154. https://doi.org/10.3832/ifor3648-014.

D'Amico, G., Chirici, C., Campetella, G., Canullo, R., Cervellini, M., Chelli, S., Di Biase, R. M., Fattorini, L., Floris, A., Franceschi, S., Francini, S., Giannetti, F., Marcelli, A., Marcheselli, M., Mattioli, W., Notarangelo, M., Papitto, G., Parisi, F., Pisani, C., Presutti Saba, E., Quatrini, V. Vangi, E., Corona P., 2025. National Forest Inventory in Italy: new perspectives for forest monitoring. Ann. For. Sci. doi: 10.1186/s13595-025-01303-9.

Dalagnol, R., Wagner, F.H., Emilio, T., Streher, A.S., Galvão, L.S., Ometto, J.P., Aragao, L.E., 2022. Canopy palm cover across the Brazilian amazon forests mapped with airborne LiDAR data and deep learning. Remote Sensing in Ecology and Conservation 8 (5), 601–614. https://doi.org/10.1002/rse2.264.

Dalponte, M., Solano-Correa, Y.T., Marinelli, D., Liu, S., Yokoya, N., Gianelle, D., 2023. Detection of forest windthrows with bitemporal COSMO-SkyMed and Sentinel-1 SAR data. Remote Sensing of Environment 297, 113787. https://doi.org/10.1016/j.rse.2023.113787.

Dubayah, RO, Armston, J, Kellner, JR, Duncanson, L, Healey, SP, Patterson, PL, Hancock, S, Tang, H, Hofton, MA, Blair, JB, 2021. GEDI L4A Footprint Level Aboveground Biomass Density, Version 1. ORNL DAAC, Oak Ridge, Tennessee, USA. Luthcke SB. https://doi.org/10.3334/ORNLDAAC/1907.

Dubayah, R, Blair, JB, Goetz, S, Fatoyinbo, L, Hansen, M, Healey, S, Hofton, M, Hurtt, G, Keller, J, Luthcke, S, Armston, J, Tang, H, Duncanson, L, Hancock, S, Jantz, P, Marseils, S, Patterson, PL, Qi, W, Silva, C, 2020. The global Ecosystem Dynamics Investigation: highresolution laser ranging of the Earth's forests and topography. Sci. Remote Sens. 1, 100002. https://doi.org/10.1016/j.srs.2020.100002.

Duncanson, L., Armston, J., Disney, M., Avitabile, V., Barbier, N., Calders, K., et al., 2019. The importance of consistent global forest aboveground biomass product validation. Surv. Geophys. 40, 979–999. https://doi.org/10.1007/s10712-019-09538-8.

Duncanson, L., Kellner, J.R., Armston, J., Dubayah, R., Minor, D.M., Hancock, S., et al., 2022. Aboveground biomass density models for NASA's global ecosystem dynamics investigation (GEDI) lidar mission. Remote Sensing of Environment 270, 112845. https://doi.org/10.1016/j.rse.2021.112845.

D'Amico, G., Francini, S., Giannetti, F., Vangi, E., Travaglini, D., Chianucci, F., Mattioli, W., Grotti, M., Puletti, N., Corona, P., Chirici, G., 2021. A deep learning approach for automatic mapping of poplar plantations using Sentinel-2 imagery. GIScience Remote Sens. 58 (8), 1352–1368. https://doi.org/10.1080/15481603.2021.1988427.

D'Amico, G., McRoberts, R.E., Giannetti, F., Vangi, E., Francini, S., Chirici, G., 2022. Effects of lidar coverage and field plot data numerosity on forest growing stock volume estimation. European Journal of Remote Sensing 55 (1), 199–212. https://doi.org/10.1080/22797254.2022.2042397.

European Commission, 2014. Annual activity report 2013: Agriculture and rural development. Publications Office of the European Union. https://ec.europa.eu/info/publications/annual-activity-report-2013-agriculture-and-rural-development.

Fayad, I., Ciais, P., Schwartz, M., Wigneron, J.P., Baghdadi, N., de Truchis, A., et al., 2024. Hy-TeC: a hybrid vision transformer model for high-resolution and large-scale mapping of canopy height. Remote Sensing of Environment 302, 113945. https://doi.org/10.1016/j.rse.2023.113945.

Feng, Y., Xu, X., Shao, H., Lu, H., Yang, R., Tang, B., 2020. Dynamics in soil quality and crop physiology under poplar-agriculture tillage models in coastal areas of Jiangsu, China. Soil Tillage Res. 204, 104733. https://doi.org/10.1016/j.still.2020.104733.

FOREST EUROPE - Liaison Unit Bratislava, 2018. Understanding the contribution of agroforestry to landscape resilience in Europe. How can policy foster agroforestry towards climate change adaptation ?.

Francini, S., D'Amico, G., Vangi, E., Borghi, C., Chirici, G., 2022. Integrating GEDI and Landsat: Spaceborne Lidar and Four Decades of Optical Imagery for the Analysis of Forest Disturbances and Biomass Changes in Italy. Sensors 22 (5), 2015. https://doi.org/10.3390/s22052015.

Freer-Smith, P.H., Muys, B., Bozzano, M., Drössler, L., Farrelly, N., Jactel, H., et al., 2019. Plantation Forests in Europe: Challenges and Opportunities, 9. European Forest Institute, Joensuu, Finland, pp. 1–52. https://doi.org/10.36333/fs09.

Gasparini, P., Di Cosmo, L., Floris, A., De Laurentis, D., 2022. Italian National Forest inventory—methods and Results of the Third Survey: Inventario Nazionale Delle Foreste E Dei Serbatoi Forestali Di carbonio—metodi E Risultati Della Terza Indagine. Springer Nature, p. 576. https://doi.org/10.1007/978-3-030-98678-0.

Giannetti, F., Chirici, G., Vangi, E., Corona, P., Maselli, F., Chiesi, M., et al., 2022. Wall-to-wall mapping of forest biomass and wood volume increment in Italy. Forests 13 (12), 1989. https://doi.org/10.3390/f13121989.

Golicz, K., Bellingrath-Kimura, S., Breuer, L., Wartenberg, A.C., 2022. Carbon accounting in European agroforestry systems–key research gaps and data needs. Current Research in Environmental Sustainability 4, 100134. https://doi.org/10.1016/j.crsust.2022.100134.

Gorelick, N., Hancher, M., Dixon, M., Ilyushchenko, S., Thau, D., Moore, R., 2017. Google Earth engine: planetary-scale geospatial analysis for everyone. Remote sensing of Environment 202, 18–27. https://doi.org/10.1016/j.rse.2017.06.031.

Guerra-Hernández, J., Pereira, J.M., Stovall, A., Pascual, A., 2024. Impact of fire severity on forest structure and biomass stocks using NASA GEDI data. Insights from the 2020 and 2021 wildfire season in Spain and Portugal. Science of Remote Sensing 9, 100134. https://doi.org/10.1016/j.srs.2024.100134.

Herold, M., Carter, S., Avitabile, V., Espejo, A.B., Jonckheere, I., Lucas, R., et al., 2019. The role and need for space-based forest biomass-related measurements in environmental management and policy. Surv. Geophys. 40 (4), 757–778. https://doi.org/10.1007/s10712-019-09510-6.

Hyde, P., Dubayah, R., Walker, W., Blair, J.B., Hofton, M., Hunsaker, C., 2006. Mapping Forest structure for wildlife habitat analysis using multi-sensor (LiDAR, SAR/InSAR, ETM+, Quickbird) synergy. Remote Sensing of Environment 102, 63–73.

Illarionova, S., Shadrin, D., Ignatiev, V., Shayakhmetov, S., Trekin, A., Oseledets, I., 2022. Estimation of the canopy height model from multispectral satellite imagery with convolutional neural networks. IEEE Access 10, 34116–34132. https://doi.org/10.1109/ACCESS.2022.3161568.

IPCC, 2006. In: Eggleston, H.S., Miwa, K., Srivastava, N., Tanabe, K. (Eds.), IPCC Guidelines for Greenhouse Gases Inventory. A Primer, Prepared by the National Greenhouse Gas Inventories Programme. IGES, Japan.

Karna, Y.K., Hussin, Y.A., Gilani, H., Bronsveld, M.C., Murthy, M.S.R., Qamer, F.M., Karky, B.S., Bhattarai, T., Aigong, X., Baniya, C.B., 2015. Integration of WorldView-2

and airborne LiDAR data for tree species level carbon stock mapping in kayar khola watershed, Nepal. Int. J. Appl. Earth Obs. Geoinf. 38, 280–291. https://doi.org/10.1016/j.jag.2015.01.011.

Kingma, D.P., Ba, J., 2014. Adam: a method for stochastic optimization. arXiv. https://doi.org/10.48550/arXiv.1412.6980.

Lang, N., Jetz, W., Schindler, K., Wegner, J.D., 2023. A high-resolution canopy height model of the Earth. Nature Ecology & Evolution 7 (11), 1778–1789. https://doi.org/10.1038/s41559-023-02206-6.

Łukaszkiewicz, J., Długoński, A., Fortuna-Antoszkiewicz, B., Fialová, J., 2024. The ecological potential of poplars (Populus L.) for city tree planting and management: a preliminary study of central Poland (warsaw) and silesia (Chorzów). Land 13 (5), 593. https://doi.org/10.3390/land13050593.

Marcelli, A., Mattioli, W., Puletti, N., Chianucci, F., Gianelle, D., Grotti, M., et al., 2020. Large-scale two-phase estimation of wood production by poplar plantations exploiting Sentinel-2 data as auxiliary information. Silva Fenn. 54 (2). https://doi.org/10.14214/sf.10247.

Moudrý, V., Prošek, J., Marselis, S., Marešová, J., Šárovcová, E., Gdulová, K., Wild, J., 2024. How to find accurate terrain and canopy height GEDI footprints in temperate forests and grasslands? Earth Space Sci. 11 (10), e2024EA003709.

Nervo, G., Bergante, S., Rosso, L., Chiarabaglio, P.M., Vietto, L., Carra, A., Giorcelli, A., Coaloa, D., Facciotto, G., Gennaro, M., Picco, F., Rizza, D., Rocci, A., Corona, P., 2024. Latest results of the breeding activity of hybrid poplars for industrial purposes in Italy. Annals of Silvicultural Research 49, 39–43. https://doi.org/10.12899/asr-2532.

Nilsson, M., Nordkvist, K., Jonzén, J., Lindgren, N., Axensten, P., Wallerman, J., et al., 2017. A nationwide forest attribute map of Sweden predicted using airborne laser scanning data and field data from the National Forest Inventory. Remote Sensing of Environment 194, 447–454. https://doi.org/10.1016/j.rse.2016.10.022.

Pauls, J., Zimmer, M., Kelly, U.M., Schwartz, M., Saatchi, S., Ciais, P., Pokutta, S., Brandt, M., Gieseke, F., 2024. Estimating canopy height at scale. arXiv preprint arXiv:2406.01076. https://doi.org/10.48550/arXiv.2406.01076.

Potapov, P., Li, X., Hernandez-Serna, A., Tyukavina, A., Hansen, M.C., Kommareddy, A., et al., 2021. Mapping global forest canopy height through integration of GEDI and Landsat data. Remote Sensing of Environment 253, 112165. https://doi.org/10.1016/j.rse.2020.112165.

Pra, A., Brotto, L., Mori, P., Buresti Lattes, E., Masiero, M., Andrighetto, N., Pettenella, D., 2019. Profitability of timber plantations on agricultural land in the Po valley (northern Italy): a comparison between walnut, hybrid poplar and polycyclic plantations in the light of the European Union Rural Development Policy orientation. Eur. J. For. Res. 138, 473–494. https://doi.org/10.1007/s10342-019-01184-4.

Puletti, N., Grotti, M., Ferrara, C., Chianucci, F., 2021. Influence of voxel size and point cloud density on crown cover estimation in poplar plantations using terrestrial laser scanning. Annals of Silvicultural Research 46 (2). https://doi.org/10.12899/asr-2256.

Romano, E., Petrangeli, A.B., Salerno, F., Guyennon, N., 2022. Do recent meteorological drought events in central Italy result from long-term trend or increasing variability? Int. J. Climatol. 42, 4111–4128. https://doi.org/10.1002/joc.7487.

Romano, E., Brambilla, M., Chianucci, F., Tattoni, C., Puletti, N., Chirici, G., Travaglini, D., Giannetti, F., 2024. Estimating canopy and stand structure in hybrid poplar plantations from multispectral UAV imagery. Ann. For. Res. 67 (1), 143–154. https://doi.org/10.15287/afr.2024.3636.

Ronneberger, O., Fischer, P., Brox, T., 2015. U-net: convolutional networks for biomedical image segmentation. In: Medical Image Computing and computer-assisted intervention–MICCAI 2015: 18Th International Conference, Munich, Germany, October 5-9, 2015, Proceedings, Part III, 18. Springer International Publishing, pp. 234–241.

Santoro, M., Cartus, O., Carvalhais, N., Rozendaal, D.M., Avitabile, V., Araza, A., et al., 2021. The global forest above-ground biomass pool for 2010 estimated from high-resolution satellite observations. Earth Syst. Sci. Data 13 (8), 3927–3950. https://doi.org/10.5194/essd-13-3927-2021.

Schelhaas, M.J., Hengeveld, G.M., Heidema, N., Thürig, E., Rohner, B., Vacchiano, G., et al., 2018. Species-specific, Pan-European diameter increment models based on data of 2.3 million trees. Forest Ecosystems 5, 1–19. https://doi.org/10.1186/s40663-018-0133-3.

Schwartz, M., Ciais, P., De Truchis, A., Chave, J., Ottlé, C., Vega, C., Wigneron, J., Nicolas, M., Jouaber, S., Liu, S., Brandt, M., Fayad, I., 2023. FORMS: forest Multiple Source height, wood volume, and biomass maps in France at 10 to 30 m resolution based on Sentinel-1, Sentinel-2, and Global Ecosystem Dynamics Investigation (GEDI) data with a deep learning approach. Earth Syst. Sci. Data 15 (11), 4927–4945. https://doi.org/10.5194/essd-15-4927-2023.

Schwartz, M., Ciais, P., Ottlé, C., De Truchis, A., Vega, C., Fayad, I., Brandt, M., Fensholt, R., Baghdadi, N., Morneau, F., Morin, D., Guyon, D., Dayau, S., Wigneron, J.P., 2024. High-resolution canopy height map in the Landes forest (France) based on GEDI, Sentinel-1, and Sentinel-2 data with a deep learning approach. Int. J. Appl. Earth Obs. Geoinf. 128, 103711. https://doi.org/10.1016/j.jag.2024.103711.

Spawn, S.A., Sullivan, C.C., Lark, T.J., Gibbs, H.K., 2020. Harmonized global maps of above and belowground biomass carbon density in the year 2010. Sci. Data 7 (1), 112. https://doi.org/10.1038/s41597-020-0444-4.

Spinelli, R., Magagnotti, N., Sperandio, G., Cielo, P., Verani, S., Zanuttini, R., 2011. Cost and productivity of harvesting high-value hybrid poplar plantations in Italy. For. Prod. J. 61 (1), 64–70. https://doi.org/10.13073/0015-7473-61.1.64.

Tauro, F., Maltese, A., Giannini, R., Harfouche, A., 2022. Latent heat flux variability and response to drought stress of black poplar: a multi-platform multi-sensor remote and proximal sensing approach to relieve the data scarcity bottleneck. Remote Sensing of Environment 268, 112771. https://doi.org/10.1016/j.rse.2021.112771.

Tolan, J., Yang, H.I., Nosarzewski, B., Couairon, G., Vo, H.V., Brandt, J., Couprie, C., 2024. Very high resolution canopy height maps from RGB imagery using self-supervised vision transformer and convolutional decoder trained on aerial lidar. Remote Sens. Environ. 300, 113888.

Tompalski, P., White, J.C., Coops, N.C., Wulder, M.A., 2019. Demonstrating the transferability of forest inventory attribute models derived using airborne laser scanning data. Remote Sensing of Environment 227, 110–124. https://doi.org/10.1016/j.rse.2019.04.006.

Torres de Almeida, C., Gerente, J., Rodrigo dos Prazeres Campos, J., Caruso Gomes Junior, F., Providelo, L.A., Marchiori, G., Chen, X., 2022. Canopy height mapping by Sentinel 1 and 2 satellite images, airborne LiDAR data, and machine learning. Remote Sens. 14, 1–21. https://doi.org/10.3390/rs14164112.

Vangi, E., D'Amico, G., Francini, S., Borghi, C., Giannetti, F., Corona, P., Chirici, G., 2023b. Large-scale high-resolution yearly modeling of forest growing stock volume and above-ground carbon pool. Environ. Modell. Softw. 159, 105580.

Vangi, E., D'Amico, G., Francini, S., Chirici, G., 2023a. GEDI4R: an R package for NASA's GEDI level 4 A data downloading, processing and visualization. Earth Sci. Inform. 16 (1), 1109–1117.

Varvia, P., Saarela, S., Maltamo, M., Packalen, P., Gobakken, T., Næsset, E., et al., 2024. Estimation of boreal forest biomass from ICESat-2 data using hierarchical hybrid inference. Remote Sensing of Environment 311, 114249. https://doi.org/10.1016/j.rse.2024.114249.

Wulder, M.A., Bater, C.W., Coops, N.C., Hilker, T., White, J.C., 2008. The role of LiDAR in sustainable forest management. For. Chron. 84 (6), 807–826. https://doi.org/10.5558/tfc84807-6.

Zanuttini, R., Negro, F., Cremonini, C., 2021. Hardness and contact angle of thermo-treated poplar plywood for bio-building. iFor. Biogeosci. For. 14 (3), 274. https://doi.org/10.3832/ifor3662-014.

Zhang, Z., Lu, L., Zhao, Y., Wang, Y., Wei, D., Wu, X., Ma, X., 2023. Recent advances in using Chinese Earth observation satellites for remote sensing of vegetation. ISPRS J. Photogrammetry Remote Sens. 195, 393–407. https://doi.org/10.1016/j.isprsjprs.2022.12.006.